

# Semi-Automatic Cell Correspondence Analysis Using Iterative Point Cloud Registration

Shuqing Chen<sup>1\*</sup>, Simone Gehrer<sup>2\*</sup>, Sara Kaliman<sup>2</sup>, Nishant Ravikumar<sup>1</sup>,  
Abdurrahman Becit<sup>1</sup>, Maryam Aliee<sup>2</sup>, Diana Dudziak<sup>3</sup>, Rudolf Merkel<sup>4</sup>,  
Ana-Sunčana Smith<sup>2,5</sup>, Andreas Maier<sup>1</sup>

<sup>1</sup>Pattern Recognition Lab, FAU Erlangen-Nürnberg, Germany

<sup>2</sup>PULS Group, Theo. Physics I, FAU Erlangen-Nürnberg, Germany

<sup>3</sup>Department of Dermatology, University Hospital Erlangen, Germany

<sup>4</sup>ICS 7: Biomechanics, Forschungszentrum Jülich GmbH, Germany

<sup>5</sup>Division of Physical Chemistry, Institute Ruder Bošković, Croatia

\*Both contributed equally.

shuqing.chen@fau.de

**Abstract.** In the field of biophysics, deformation of *in-vitro* model tissues is an experimental technique to explore the response of tissue to a mechanical stimulus. However, automated registration before and after deformation is an ongoing obstacle for measuring the tissue response on the cellular level. Here, we propose to use an iterative point cloud registration (IPCR) method, for this problem. We apply the registration method on point clouds representing the cellular centers of mass, which are evaluated with a Watershed based segmentation of phase-contrast images of living tissue, acquired before and after deformation. Preliminary evaluation of this method on three data sets shows high accuracy, with 82 % - 92 % correctly registered cells, which outperforms coherent point drift (CPD). Hence, we propose the application of the IPCR method on the problem of cell correspondence analysis.

## 1 Introduction

Epithelial and other types of tissues are constantly exposed to stress, which is affecting the cell shape. The mechanism of this response is not understood, and progress lies on deconvolving the response of individual cells comprising the tissue. This requires sophisticated and automated image analysis techniques. Here, we induce an affine deformation of a 2D tissue model to relate the macroscopic deformation of the tissue to changes on the cellular level for a large number of cells in an automated fashion.

In our experiments, MDCK II cells (Madin Darby Kidney Cells) were grown as confluent epithelial cell layers on fibronectin(FN)-coated Polydimethylsiloxane (PDMS), and subjected to uniaxial stress through the underlying substrate. With existing methods it is only possible to investigate the average cell shape changes in the distributions over all cells for large tissue deformations. However, establishing the correspondence of every single cell is not yet possible for statistical relevant sample sizes.

The cell correspondence problem can also be formulated as a cell tracking problem, which often relies on cell detection based on computer vision algorithms [1, 2] and a series of time frames as input. However, image registration has been seldom employed for this purpose. Nonetheless, recent studies showed that image registration is potent for aligning cell nuclei [3] and feasible for tracking of single cells imaged with phase-contrast [4].

In this work, we propose a novel approach based on Watershed segmentation and iterative point cloud registration (IPCR), to find the cellular correspondences in the micrographs before and after deformation, such that shape changes may be investigated for each cell independently. By this we present, to the best of our knowledge, the first cell correspondence analysis algorithm using point cloud registration.

## 2 Materials and methods

### 2.1 Cell stretching and image acquisition

Clusters of MDCK II monolayers (about 8,000 cells) were stretched using FN-coated PDMS substrates and a cell-stretching device [5] (Fig. 1a). Samples were imaged before and subsequently after deformation in phase-contrast tile scans (Axiovert 200M, 10 $\times$ /0.25 Achroplan, both Zeiss, pixel size: 0.8 $\mu$ m  $\times$  0.8 $\mu$ m)[6]. Resulting images were background corrected [7] and stitched using ImageJ [8].

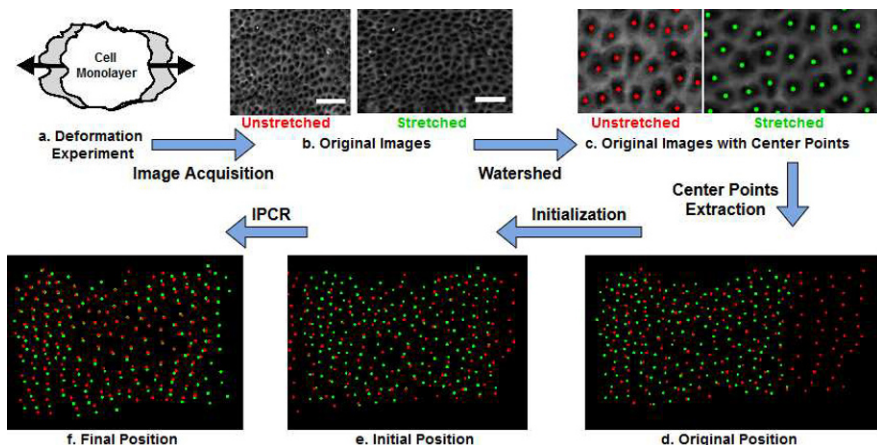


**Fig. 1.** The workflow of the proposed approach. a) Scheme of the deformation experiment. b) The original images, left: unstretched; right: stretched for 30 %. Scale bar 50  $\mu$ m. c) Zoomed-in images with center points. d) Original position of the two point clouds. e) Initial position after manual placement. f) Best matching after the registration. The unstretched and the stretched images are denoted with red and green, respectively.

## 2.2 Semi-automatic cell correspondence analysis

The workflow of the proposed approach to the cell correspondence analysis problem is illustrated in Fig. 1. The approach consists of two steps, elaborated below: (i) Cell centroid coordinates before and after stretching are obtained by segmentation. These centroids represent the images as point clouds, for subsequent steps. (ii) The spatial relationship of the point clouds is initialized by manual placement using a visual representation. Finally, we obtain the spatial relationship and therefore, cellular correspondence using IPCR.

**Cell segmentation** Cell segmentation is implemented using MATLAB [9]. As an input, the program can take either an image of a cell monolayer or a stitched image showing a whole cell cluster.

1. If the input is a whole cell cluster, the edge of the cluster is found using Otsu's method [10], so that single cells and dirt outside the cluster are excluded. Within the current imaging approach slightly lower threshold levels (90 % of the calculated level) provided the best outline of the cell cluster (Fig. 2a).
2. Small objects as well as the holes in the cell layer are removed by the area-opening-procedure. The border of the cell cluster is recognized using a flood-fill algorithm and used as a mask for further image analysis.
3. For the segmentation of single cell shapes within the mask, we used the Watershed algorithm, which can be applied since cell-cell contacts appear brighter in the image. After applying H-minima transformation to suppress all insignificant minima in the image, we obtain the watershed lines using the Fernand Meyer algorithm [11].
4. Cells are recognized as different objects with the flood-fill algorithm, and their center of mass is calculated assuming the same weight of each pixel (Fig. 2 b). Objects which are too small to be a cell (deviate more than two standard deviations from the mean cell area value) are removed.

**Iterative point cloud registration** As described previously, the cell correspondences should be obtained based on the clouds of the extracted center points. Fig. 3 shows the flowchart of our registration algorithm. The algorithm is described in the following:

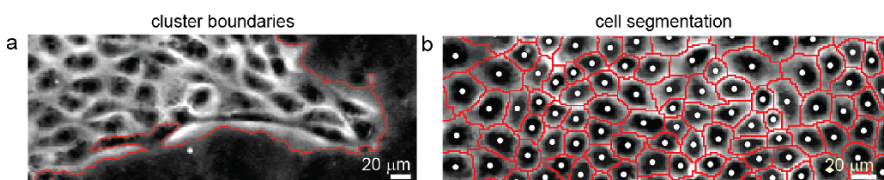


**Fig. 2.** Segmentation results. a) Segmented border (red) of a typical cell cluster. b) Cell segmentation (red) and corresponding centers of cell mass (white dots).

1. With a visualization of the extracted 2D point clouds assuming  $\mathbf{A} = \{\mathbf{a}_1, \dots, \mathbf{a}_M\}$  as the source and  $\mathbf{B} = \{\mathbf{b}_1, \dots, \mathbf{b}_N\}$  as the target or the reference, an initial position  $\mathbf{T}^0$  is obtained manually by moving the source cloud close to the target cloud.
2. The initial point matching  $\mathbf{A}_c^0$  and  $\mathbf{B}_c^0$  is generated according to the initial transformation  $\mathbf{T}^0$  based on  $k$ -d tree nearest neighbor (NN) search [12]. Due to the outlier rejection in the NN search, the matched point clouds are equal to or smaller than the original point clouds, i.e.  $\mathbf{A}_c \subseteq \mathbf{A}$  and  $\mathbf{B}_c \subseteq \mathbf{B}$ .
3. The transformation matrix  $\mathbf{T}$  is updated to achieve optimal alignment of the two reciprocal point clouds  $\mathbf{A}_c$  and  $\mathbf{B}_c$ .
4. The point matching is recalculated using the new transformation matrix.
5. Step 3 and Step 4 are repeated until the termination criterion is fulfilled.

We used the Fast Library for Approximate Nearest Neighbors (FLANN) [12] for the  $k$ -d tree NN search. Covariance Matrix Adaptation Strategy (CMA-ES) [13] is utilized as the optimizer to update the transformation between the point clouds. Because the image was stretched, we assumed that the transformation is affine and the variation can be constrained with translation and scaling. The cost function of our optimization problem is defined with Euclidean distances of the reciprocal points (Eq. 1). We also used the average Euclidean distance in the termination criterion of the iterative algorithm to determine whether the best point matching is achieved

$$f = \frac{M \cdot N}{K^3} \sum_{k=1}^K \|\mathbf{T} \cdot \mathbf{a}_{c,k} - \mathbf{b}_{c,k}\| \quad (1)$$

where  $K$  is the amount of the reciprocal pairs,  $M$  and  $N$  are the number of points of the source and the target,  $K \leq M$  and  $K \leq N$ .

### 3 Results

The proposed approach for cell correspondence analysis was evaluated with three data sets. Each data set contains two images before and after the deformation (Fig. 1b). Tab. 1 summarizes the information of the evaluated results of these three data sets. Cells (U/S) records the total number of cells of the unstretched (U) and stretched (S) images. The proposed approach is compared with another major type of point cloud registration algorithm – the coherent point drift (CPD) algorithm [14]. *Found* shows the calculated correspondences using FLANN [12]

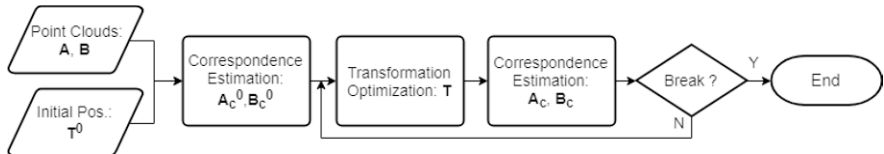


**Fig. 3.** Flowchart of the proposed IPCR method.

**Table 1.** Information and results of the evaluated data sets.

| Data  | Cells<br>(U/S) | deform. | CPD [14]     |               |             | Proposed     |               |             |     |      |
|-------|----------------|---------|--------------|---------------|-------------|--------------|---------------|-------------|-----|------|
|       |                |         | found<br>[%] | eval.<br>cor. | Acc.<br>[%] | found<br>[%] | eval.<br>cor. | Acc.<br>[%] |     |      |
| Set 1 | 160/156        | 30.0 %  | 91.0         | 142           | 137         | 87.8         | 91.0          | 142         | 140 | 89.7 |
| Set 2 | 170/158        | 20.3 %  | 86.1         | 136           | 52          | 32.9         | 92.4          | 146         | 145 | 91.8 |
| Set 3 | 1264/900       | 20.3 %  | 88.2         | 301           | 69          | 20.2         | 88.4          | 289         | 267 | 81.7 |

after the registration in percentage of the maximum of possible correspondences. Eval. and correct records the number of evaluated pairs, and out of those the correctly identified ones. The proposed approach obtained 88.4 %–92.4 % reciprocal cell pairs. The calculated accuracy, according to Eq. 2, is 81.7 %–91.8 %

$$\text{Acc.} = \text{found} \times \frac{\text{Correct correspondences}}{\text{Evaluated cells}} \quad (2)$$

## 4 Discussion

We propose a novel approach based on the Watershed algorithm and IPCR to identify correspondences in the practical analysis of cells in tissue. We report 81.7 % to 91.8 % of correctly aligned cells in the preliminary evaluation and outperform CPD (with default parameter settings), which suggests that our approach is feasible for cell correspondence analysis. For the data set 1 with 30 % deformation, both methods performed similarly. Comparing the registration of different sized data sets (2 and 3), the proposed method obtained more correct reciprocal cell pairs in both cases. An important observation is that CPD provides high accuracy at the center of the input, declining with the distance to the center. The reason could be that CPD supposes the point sets are distributions built by a Gaussian Mixture Model (GMM). This may be due the manual initialization used in this study and the uniform distribution term incorporated within the GMM by CPD, designed to accommodate outliers and missing correspondences. However, minimal missing correspondences and outliers were present in the data used in this study. Consequently, CPD is inferred to over-constrain the registration process, and the here proposed approach thus resulted in higher accuracy.

It is important to note that only a baseline is provided in this work. Currently, the deformation is assumed to be affine, as appropriate for the given experiment, where only translation and scaling are considered. Rotation and elastic deformation could also be considered for more complex problems, which could be particularly relevant for tissues that exhibit large deformations or strong restructurings of the cell neighborhoods. The optimization and termination could be further improved by using the information on cell area and its connectivity to other cells. Furthermore, the manual initialization could be replaced by an automatic method, which would be useful for large data sets. For the analysis

of tissues over long time scales, the algorithm should be augmented to account for cell death and division (i.e. missing correspondences). In the context of these challenges, image registration seems a particularly suitable approach.

**Acknowledgement.** This work has partly been supported by the European Research Council to ASS (ERC StG 2013-337283, MEMBRANESACT), by the German Research Foundation to ASS and DD (RTG 1962), and by the Emerging Field Initiative of the FAU Erlangen-Nürnberg: Big-Thera to AM, ASS and DD.

## References

1. Mualla F, Schöll S, Sommerfeldt B, et al. Automatic cell detection in bright-field microscope images using SIFT, random forests, and hierarchical clustering. *IEEE Trans Med Imaging*. 2013;32(12):2274–2286.
2. Mualla F, Schöll S, Sommerfeldt B, et al. Unsupervised unstained cell detection by SIFT keypoint clustering and self-labeling algorithm. *Med Image Comput Comput Assist Interv*. 2014; p. 377–384.
3. De Vylder J, De Vos WH, Manders EM, et al. 2D mapping of strongly deformable cell nuclei-based on contour matching. *Cytometry A*. 2011;79A(7):580–588.
4. Hand A, Sun T, Barber D, et al. Automated tracking of migrating cells in phase-contrast video microscopy sequences using image registration. *J Microsc*. 2009;234(1):62–79.
5. Faust U, Hampe N, Rubner W, et al. Cyclic stress at mHz frequencies aligns fibroblasts in direction of zero strain. *PLoS One*. 2011;6(12):e28963.
6. Gehrer S. Stress-strain relation in reconstituted tissue. Friedrich-Alexander-Universität Erlangen-Nürnberg; 2016.
7. Sternberg SR. Biomedical image processing. *Comput*. 1983;16:22 – 34.
8. Preibisch S, Saalfeld S, Tomancak P. Globally optimal stitching of tiled 3D microscopic image acquisitions. *Bioinform*. 2009;25(11):1463.
9. Kaliman S, Jayachandran C, Rehfeldt F, et al. Limits of applicability of the voronoi tessellation determined by centers of cell nuclei to epithelium morphology. *Front Physiol*. 2016;7.
10. Otsu N. A threshold selection method from gray-level histograms. *IEEE Trans Syst Man Cybern*. 1979;9(1):62–66.
11. Meyer F. Topographic distance and watershed lines. *Sign Process*. 1994;38(1):113 – 125.
12. Muja M, Lowe DG. Fast approximate nearest neighbors with automatic algorithm configuration. *VISAPP*. 2009; p. 331–340.
13. Hansen N. The CMA evolution strategy: a comparing review. *Towards New Evol Comput*. 2006; p. 75–102.
14. Myronenko A, Song X. Point set registration: coherent point drift. *IEEE Trans Pattern Anal Mach Intell*. 2010;32(12):2262–2275.